Archives of Materials Science and Engineering

Volume 127
Issue 1
May 2024
Pages 5-11

International Scientific Journal
published monthly by the
World Academy of Materials
and Manufacturing Engineering

DOI: 10.5604/01.3001.0054.7244

Determination of borides in Fe-Mo-B sintered powders using diffraction methods

J. Karwan-Baczewska [a], M. Perek-Nowak [a,*], M. Majchrowska [a], A. Garbacz-Klempka [b]

[a] Faculty of Non-Ferrous Metals, AGH University, Al. A. Mickiewicza 30, 30-059 Kraków, Poland
[b] Faculty of Foundry, AGH University, ul. Reymonta 23, 30-059 Kraków, Poland
* Corresponding e-mail address: mperek@agh.edu.pl
ORCID identifier: https://orcid.org/0000-0003-0323-1624 (M.P.-N.)

ABSTRACT

Purpose: Modification of sintered iron with the addition of molybdenum and boron leads to the formation of boride phases that significantly impact the properties of the sintered materials. The paper aims to determine Fe-Mo-B phases that might be formed during the sintering of base powders. With EDS microanalysis, determining those phases in the microstructure is difficult since the B-Kα peak is extremely close to Mo-Mζ (only a 9.3 eV difference). Thus, diffraction techniques must be implemented to unambiguously define the phases occurring in the sintered samples (WDS and EBSD).

Design/methodology/approach: The sintered samples were obtained from initial powders of Fe, Mo, and B that were mixed and compressed. The reducing hydrogen atmosphere was used to sinter green samples at 1200°C for 60 minutes. The obtained sinters were subjected to microstructural observations by scanning electron microscope, and some analyses (EDS/WDS and EBSD) were conducted, which led to the determination of phases present in the material.

Findings: Based on the investigations conducted, iron, molybdenum, and molybdenum-iron borides have been reported. It is confirmed with the EBSD method that Fe_2B, MoB and $FeMo_2B_2$ phases are formed in particles' connection regions. Besides, the interparticle region, formed due to a liquid phase during sintering, is based on Fe-Fe_2B eutectic. The microstructural observations prove that the amount of the liquid phase, and thus the size of the interparticle region, diminishes with increasing molybdenum content. It was also noted that the iron matrix (interior of former iron particles) is free from contributing elements coming from boron or molybdenum powders.

Research limitations/implications: The application of the EDS method is limited in the case of measuring boron in Mo-containing alloys and phases. The EDS method does not have a sufficient energetic resolution to separate the B-Kα line from Mo-Mζ one. Thus, it must be complemented with WDS and EBSD in order to unambiguously determine the presence and localization of iron and molybdenum borides.

Practical implications: It can be stated that WDS has sufficient energy resolution to separate B-Kα from Mo-Mζ emission lines. Therefore, WDS analysis is suitable for boride observation in sintered iron powders by constructing distribution maps of interparticle connection regions and precipitates. Besides, measurements by the EBSD method can be used to confirm the presence of Fe_2B, MoB and $FeMo_2B_2$ phases.

Originality/value: Determination of boron-containing phases in Fe-Mo-B sinters by means of diffraction methods.

Keywords: Composites, Non-destructive testing, Activated sintering, Fe-Mo-B sinters, WDS, EBSD

Reference to this paper should be given in the following way:

J. Karwan-Baczewska, M. Perek-Nowak, M. Majchrowska, A. Garbacz-Klempka, Determination of borides in Fe-Mo-B sintered powders using diffraction methods, Archives of Materials Science and Engineering 127/1 (2024) 5-11. DOI: https://doi.org/10.5604/01.3001.0054.7244

MATERIALS

1. Introduction

Activated sintering can be regarded as one of the simpler methods to increase the density of produced steel parts. The overview of many sintering processes, including the one crucial to obtaining samples described in this paper, can be found there [1]. According to [1], sintering with a liquid phase occurs at "a temperature above the melting point of the lowest fusible of at least two powders forming the mixture".

Madan and German were the first researchers to study activated sintering initiated by boron addition in iron alloys [2]. Usually, sintering that involves a liquid phase occurs in multi-component systems of pre-alloyed powders or mixtures of elemental powders, as they guarantee the presence of low melting eutectics [1]. Similarly, boron added to iron and iron-based powder mixtures enhances sintering with the presence of a liquid phase by decreasing the sintering temperature down to 1200°C or even 1175°C in iron-based sinters to 1000°C in steel-based ones [2-22]. Simultaneously, diffusion processes are activated, enhancing the sintering process in the solid state. Additionally, boron improves eutectic formation on interparticle boundaries [2,4, 7-10, 13,15, 21-22]. The thermodynamic approach, including regions of phase diagram where various borides can be formed, is presented in [20-23].

Moreover, as an extra remark, it can be mentioned that a pre-alloyed Fe-Mo-B powder mixture was sometimes added to 316L steel powder to enhance sintering by forming a liquid phase between steel particles [12]. In the mentioned paper, the sintering process was conducted in a temperature range of 1200-1350°C, leading to considerable densification.

The mechanical properties of sintered iron, iron alloy or steels with boron were analysed in [5, 8-10, 14-17], while the explanation of the sintering mechanism for these alloys can be found in [21,22]. Additionally, in Fe-Mo-B sinters with the increasing Mo content (3-5%), the amount of the liquid phase at grain boundaries decreases. At the same time, larger quantities of molybdenum borides and carboborides evolve in the microstructure [16].

The main motivation for the studies was the determination of the phases formed in the sintered material of iron, molybdenum and boron powders. It was suspected from previous thermodynamic analyses [21] that the following phases might be formed during the sintering: Fe_2B, $FeMo_2B_2$, and MoB with ferritic iron in the matrix. However, structural investigations involving diffraction methods had to be involved in order to 1) localise boron in the interparticle regions and the newly formed phases (WDS) and 2) unambiguously define these phases (by means of EBSD). The crystal structures of Mo_2B_5 and MoB_2 compounds are described in [24,25].

The main issue that prompted us to use WDS analysis was the close location of spectral lines of characteristic radiation for B-Kα and Mo-Mζ; only a 9.3 eV difference. Such a small difference is beyond the energetic resolution of the standard EDS method. However, WDS seems to be designed to help differentiate them. The problem of determining the elements that exist in the same phase is presented in [26,27].

2. Experimental method

Samples with two concentrations of molybdenum (2 and 3wt. % Mo) and four concentrations of boron (0, 0.2, 0.4, and 0.6% B) were chosen for the experiments. The larger investigations included a broader range of Mo concentration from 0 to 5wt %; for the properties of such sinters, it is advised to look into the following papers [13,16,18].

The micrographs (secondary electrons, SE) of the initial powders were taken at Hitachi S-3400N scanning electron microscope (SEM) at an accelerating voltage of 10kV. The morphology of the used powders is presented in Figure 1; the iron powder is spongy-like in character, molybdenum powder is an aggregate of smaller and larger crystallites, while boron powder is flaky and also has a tendency to

agglomerate. Powder mixtures underwent mixing in a Turbula mixer and were compacted at a pressure of 600 MPa. The sintering proceeded at a temperature of 1200°C for 60 minutes in a hydrogen atmosphere.

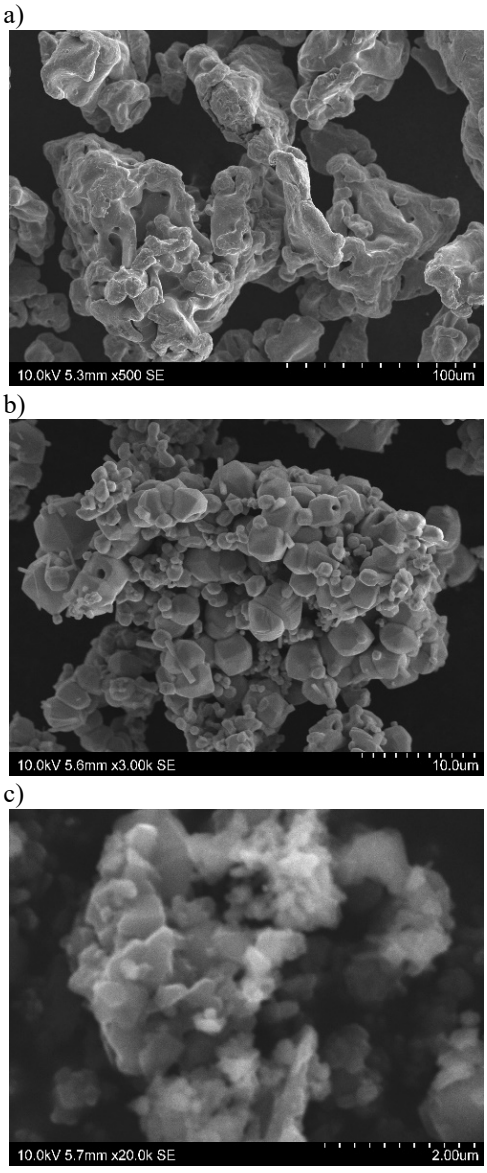

Fig. 1. Secondary electron micrographs of powders used for sintering samples a) iron, magnification 500x, b) molybdenum, 3000x, c) boron, 20 000x

The sinters with the concentrations selected for the paper exhibited well-developed eutectic zones in interparticle regions due to the formation of a considerably large amount of a liquid phase during sintering. The regions were suspected of the presence of both Fe and Mo borides. Additionally, block precipitates of the Mo borides were distributed in the microstructure. It was noted that with the increase of Mo content, more block borides are present with the cost of eutectics between the iron particles [16].

The shape of the sintered samples was square in cross-section with dimensions 5x5 mm. All the samples were polished at sand papers 500 to 4000, diamond paste 1μm, and the final polishing was with colloidal silica.

The specimens were observed at SEM Hitachi Su-70 equipped with energy dispersive X-ray spectrometry (EDS) and wavelength dispersive X-ray spectrometry (WDS) detectors, both produced by Thermo Noran. For the WDS analysis of boron, the NiC80 diffracting crystal was chosen. The applied accelerating voltage was 10 kV for surface observations and EDS/WDS (Energy Dispersive Spectrometry and Wavelength Dispersive Spectrometry) analyses.

Additionally, electron backscattered diffraction (EBSD) measurements were carried out to unambiguously determine the present borides. The used SEM was Tescan Mira, which was equipped with an EBSD detector by Oxford Instruments. The applied accelerating voltage for analyses was 20 kV.

3. Results and discussion

During the sintering of Fe-Mo-B powders, a considerable amount of liquid phase is formed in spaces between iron particles (Figs. 2 and 3). The connection is quite accurate, where the liquid phase fills completely interparticle regions with little or no visible porosity. The solidified liquid phase consists of an eutectic solution made of Fe-Fe_2B, with some regions enriched in molybdenum (Figs. 2d, 3d). The image representing such a situation in two compositions of powder mixtures Fe-2Mo-0.4B and Fe-2Mo-0.6B are shown in Figures 2 and 3, respectively. The bright needle-like regions in the SE image (Fig. 2a) is a Mo-B phase (compare elemental distribution maps in Fig. 2b with Figs. 2c, d).

The connection region between four particles in Fe-2Mo-0.6B is presented in Figure 3. The microstructure has an eutectic character comprising regions with Fe, iron boride, and Fe-Mo-B phases. The microstructure of the Fe-2Mo-0.6B sinter is like that of Fe-2Mo-0.4B. However, it differs from the microstructure reported for sinters with higher concentrations of Mo. It is noted that with increasing Mo content, the amount of liquid phase decreases with the simultaneous formation of large block crystals of $FeMo_2B_2$, e.g. Fe-3Mo-0.6B sinter in Figure 4. In such a case, the regions demonstrating eutectic can still be found; however,

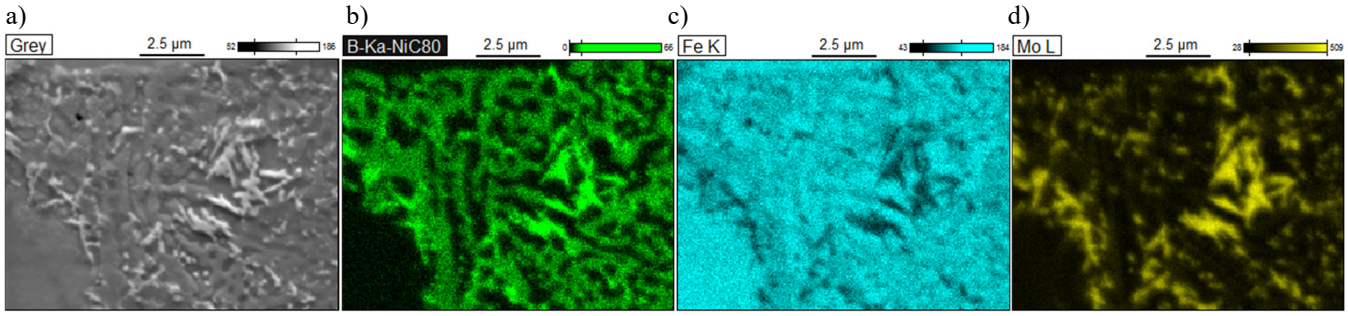

Fig. 2. Interparticle region in Fe-2Mo-0.4B sample: a) SE image of the observed surface, b) boron distribution measured with WDS, c) iron distribution measured with EDS, d) molybdenum distribution measured with EDS

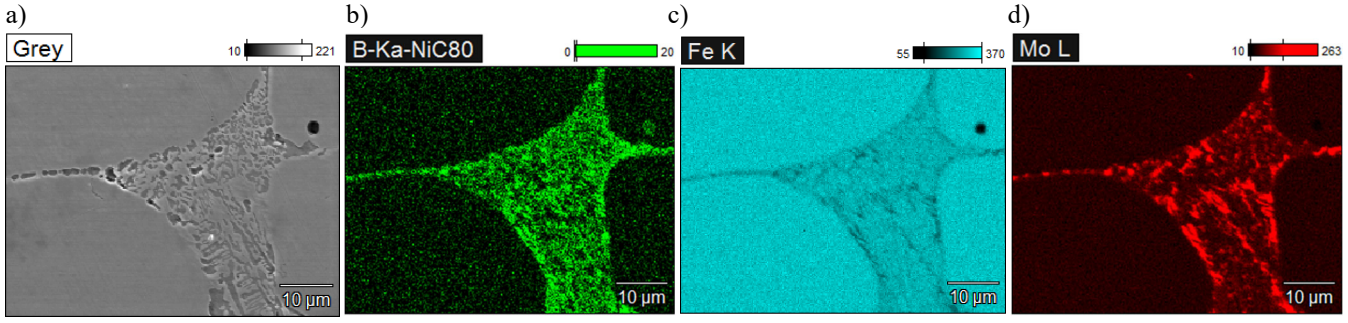

Fig. 3. Interparticle region in Fe-2Mo-0.6B sample: a) SE image of the observed surface, b) boron distribution measured with WDS, c) iron distribution measured with EDS, d) molybdenum distribution measured with EDS

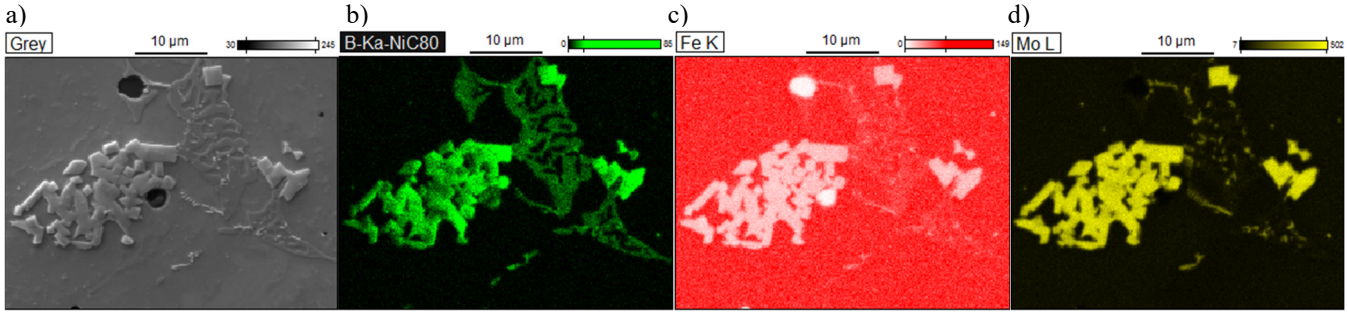

Fig. 4. Microstructure of Fe-3Mo-0.6B sample: a) SE image of the observed surface, b) boron distribution measured with WDS, c) iron distribution measured with EDS, d) molybdenum distribution measured with EDS

their amount is smaller and narrower. The microregion studies and analyses have never shown places with pure molybdenum or boron. Thus, it is concluded that all Mo powder has reacted, forming borides. Similarly, boron, a highly reactive element, reacted with iron or molybdenum.

A similar situation is observed in sinters with higher molybdenum content (3%Mo). However, more $FeMo_2B_2$ phases in the form of regular block precipitates can be observed. Additionally, there is a tendency to decrease the amount of eutectic regions in between particles as the Mo content increases [16]. Figure 4 presents this larger amount of Fe and Mo borides, often grouped together in the microstructure and eutectic region made of Fe_2B and Fe in the bcc crystal structure.

The EBSD analysis provides valuable information on phases present in the microstructure of Fe-2Mo-0.4B (Fig. 5). In the SE micrograph, there are inserted points where certain phase was determined. The exemplary

Kikuchi patterns for respective phases are presented in additional images (Fig. 6a-d). The colour is assigned to the found phases so that the point marked in the microstructure corresponds to the simulation of the diffraction pattern imposed on a raw Kikuchi pattern obtained: Fe is marked with magenta, Fe_2B – dark blue, $FeMo_2B_2$ – red, and MoB – yellow.

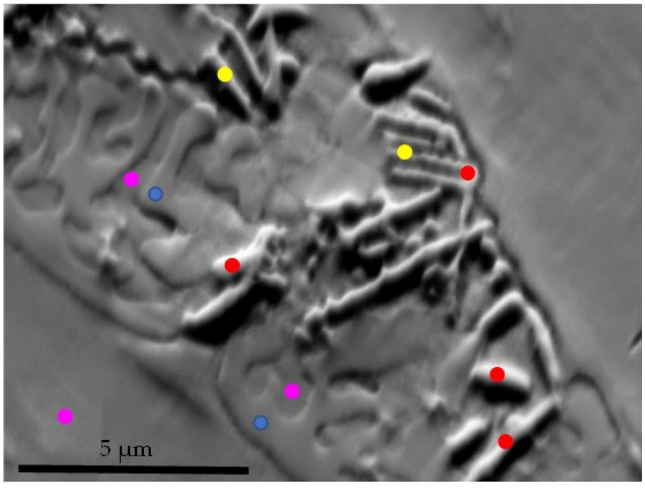

Fig. 5. SE image with marked points of EBSD measurement of Kikuchi patterns; colours correspond to detected phases: magenta is Fe bcc, blue is Fe_2B, red is $FeMo_2B_2$, and yellow is MoB; presented in Figure 6

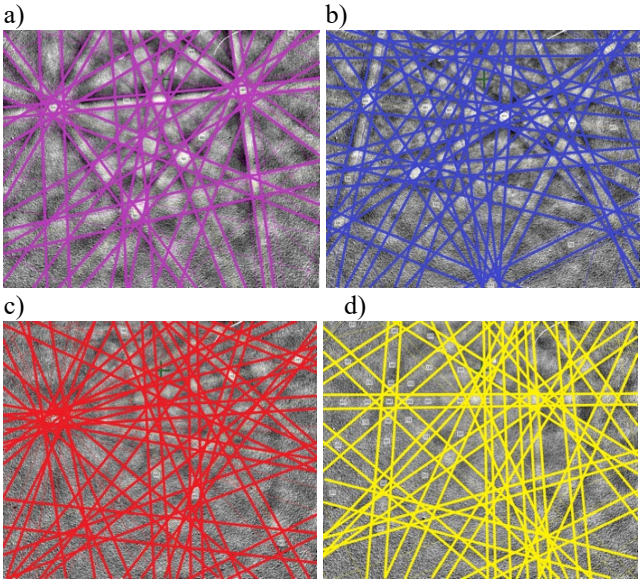

Fig. 6. Examples of Kikuchi patterns for the determined phases marked with the same colours in Figure 5: a) Fe bcc, b) Fe_2B, c) $FeMo2B_2$, d) MoB

4. Conclusions

Based on the conducted investigations, the following results can be presented

1. Presence of iron, molybdenum and molybdenum-iron borides is reported
2. WDS has sufficient energy resolution to separate B-Kα from Mo-Mζ emission lines
3. WDS analysis is suitable for borides observation and construction of distribution maps in sintered iron powders
4. The presence of Fe_2B, MoB and $FeMo_2B_2$ phases in particles' connection regions is confirmed with the EBSD method
5. The iron matrix (interior of former iron particles) is free from contributing elements coming from boron or molybdenum powders.

Research funding

The financial support of AGH University of Science and Technology under statutory funds grant no. 16.16.180.006 is acknowledged.

References

[1] L.A. Dobrzański, L.B. Dobrzański, A.D. Dobrzańska-Danikiewicz Overview of conventional technologies using the powders of metals, their alloys and ceramics in Industry 4.0 stage, Journal of Achievements in Materials and Manufacturing Engineering 98/2 (2020) 56-85.
DOI: https://doi.org/10.5604/01.3001.0014.1481

[2] D.S. Madan, R.M. German, Enhanced sintering of iron alloyed with B, C, P, Mo, Ni, Proceedings of International PM Conference, Germany, Düsseldorf, 1986, 2, 1223-1226.

[3] M. Sarasola, T. Gomez-Acebo, F. Castro, Liquid generation during sintering of Fe-3.5%Mo powder compacts with elemental boron, Acta Materialia 52/15 (2004) 4615-4622.
DOI: https://doi.org/10.1016/j.actamat.2004.06.018

[4] M. Sarasola, C. Tojal, F. Castro, Study of boron behavior during sintering of Fe/Mo/B/C alloys to near full density, Proceedings of the Euro PM2004 Conference, Austria, Vienne, 2004, 3, 319-326.

[5] R. Bolina, R.M. German, Supersolidus sintering of boron doped stainless steel powder compacts, Proceedings of the Euro PM2004 Conference, Austria, Vienne, 2004, 3, 341-348.

[6] J. Karwan-Baczewska, Boron influence on the liquid phase sintering and mechanical properties of P/M Distalloy alloys, Proceedings of the Advanced Powder Metallurgy and Particulate Materials, 1996, 3, (11-15)-(11-27).
[7] M.V. Sundaram, K.B. Surreddi, E. Hryha, A. Veiga, S. Berg, F. Castro, L. Nyborg, Enhanced Densification of PM Steels by Liquid Phase Sintering with Boron-Containing Master Alloy, Metallurgical and Materials Transactions A 49 (2018) 255-263. DOI: https://doi.org/10.1007/s11661-017-4383-4
[8] J. You, H.G. Kim, J. Lee, K. Kang, H.M. Lee, M. Kim, S.-H. Hong, Microstructure Modification of Liquid Phase Sintered Fe-Ni-B-C Alloys for Improved Mechanical Properties, Metallurgical and Materials Transactions A 52 (2020) 4395-4401. DOI: https://doi.org/10.1007/s11661-021-06392-5
[9] M. Nakamura, K. Kamada, Influence of the Addition of Boron on the Sintering Temperature and the Mechanical Properties of P/M Type Stainless Steels, Journal of the Japan Society of Powder Metallurgy 38/1 (1991) 22-26. DOI: https://doi.org/10.2497/jjspm.38.22
[10] H. Kuroki, A Review on the Effect and Behaviour of Boron in Sintered Iron and Steel, Journal of the Japan Society of Powder Metallurgy 48/4 (2001) 293-304. DOI: https://doi.org/10.2497/jjspm.48.293
[11] J. Liu, A. Cardamone, T. Potter, R.M. German, F.J. Semel, Liquid phase sintering of iron–carbon alloys with boron additions, Powder Metallurgy 43/1 (2000) 57-61. DOI: https://doi.org/10.1179/pom.2000.43.1.57
[12] X. Yang, S. Guo, Fe-Mo-B Enhanced Sintering of P/M 316L Stainless Steel, Journal of Iron and Steel Research, International 15/1 (2008) 10-14. DOI: https://doi.org/10.1016/S1006-706X(08)60003-5
[13] J. Karwan-Baczewska, The properties and structure of boron modified P/M iron-molybdenum alloys, Archives of Metallurgy 46/4 (2001) 439-445.
[14] J. Karwan-Baczewska, Processing of Distaloy SA sintered alloys with boron and carbon, Archives of Metallurgy and Materials 60/1 (2015) 41-45. DOI: https://doi.org/10.1515/amm-2015-0006
[15] J. Karwan-Baczewska, The properties of Fe-Ni-Mo-Cu-B materials produced via liquid phase sintering, Archives of Metallurgy and Materials 56/3 (2011) 789-796. DOI: https://doi.org/10.2478/v10172-011-0087-8
[16] J. Karwan-Baczewska, M. Rosso, Effect of Boron on microstructure and mechanical properties of PM sintered and nitrided steels, Powder Metallurgy 44/3 (2001) 221-227. DOI: https://doi.org/10.1179/003258901666374
[17] M. Selecká, A. Šalak, H. Danninger, The effect of boron liquid phase sintering on properties of Ni-, Mo- and Cr-alloyed structural steels, Journal of Materials Processing Technology 143-144 (2003) 910-915. DOI: https://doi.org/10.1016/j.jmatprotec.2003.10.001
[18] M. Perek-Nowak, J. Karwan-Baczewska, Influence of molybdenum and boron addition on fracture of P/M parts, Key Engineering Materials 682 (2016) 265-269. DOI: https://doi.org/10.4028/www.scientific.net/KEM.682.265
[19] Z.A. Duriagina, M.R. Romanyshyn, V.V. Kulyk, T.M. Kovbasiuk, A.M. Trostianchyn, I.A. Lemishka, The character of the structure formation of model alloys of the Fe-Cr-(Zr, Zr-B) system synthesized by powder metallurgy, Journal of Achievements in Materials and Manufacturing Engineering 100/2 (2020) 49-57. DOI: https://doi.org/10.5604/01.3001.0014.3344
[20] M. Sarasola, T. Gomez-Acebo, F. Castro, Microstructural development during liquid phase sintering of Fe and Fe-Mo alloys containing elemental boron additions, Powder Metallurgy 48/1 (2005) 59-67. DOI: https://doi.org/10.1179/003258905X37558
[21] J. Karwan-Baczewska, B. Onderka, Sintering prealloyed powders Fe-Ni-Cu-Mo modified by boron base on thermodynamic investigations, in: L.A. Dobrzański (ed), Powder Metallurgy – Fundamentals and Case Studies, IntechOpen, Rijeka, 2017, 29-53. DOI: https://doi.org/10.5772/66875
[22] E. Dudrova, M. Selecká, R. Bureš, M. Kabátová, Effect of Boron Addition on Microstructure and Properties of Sintered Fe-1.5Mo Powder Materials, ISIJ International 37/1 (1997) 59-64. DOI: https://doi.org/10.2355/isijinternational.37.59
[23] A. Molinari, T. Pieczonka, J. Kazior, S. Gialanella, G. Straffelini, Dilatometry Study of the Sintering Behavior of Boron-Alloyed Fe-1.5 Pct Mo Powder, Metallurgical and Materials Transactions A 31 (2000) 1497-1506. DOI: https://doi.org/10.1007/s11661-000-0160-9
[24] M. Frotscher, W. Klein, J. Bauer, C.-M. Fang, J.-F. Halet, A. Senyshyn, C. Baehtze, B. Albert, M_2B_5 or M_2B_4? A Reinvestigation of the Mo/B and W/B System, Zeitschrift für anorganische und allgemeine Chemie 633/15 (2007) 2626-2630. DOI: https://doi.org/10.1002/zaac.200700376
[25] D.V. Rybkovskiy, A.G. Kvashnin, Y.A. Kvashnina, A.R. Oganov, Structure, Stability, and Mechanical Properties of Boron-Rich Mo−B Phases: A Computational Study, Journal of Physical Chemistry Letters 11/7 (2020) 2393-2401. DOI: https://doi.org/10.1021/acs.jpclett.0c00242

[26] H. Dijkstra, P. Kellner, W. Reichstein, U. Glatzel, The analysis of Mo_5SiB_2 in the SEM with the use of EDS and WDS, Proceedings of the European Microscopy Congress, 2016, 957-958. DOI: https://doi.org/10.1002/9783527808465.EMC2016.6926

[27] P.M. Kellner, H. Dijkstra, U. Glatzel, Quantitative analysis of Mo–Si–B alloy phases with wavelength dispersive spectroscopy (WDS–SEM), X-Ray Spectrometry 47/2 (2018) 153-158. DOI: https://doi.org/10.1002/xrs.2824